A neurogenic perspective of sarcopenia: time course study of sciatic nerves from aging mice

Vidya S. Krishnan, MSc; Zoe White, BSc (Hons); Chris D. McMahon, PhD; Stuart I. Hodgetts, PhD; Melinda Fitzgerald, PhD; Tea Shavlakadze, PhD; Alan R. Harvey, PhD and Miranda D. Grounds, PhD

From the School of Anatomy, Physiology and Human Biology, The University of Western Australia, Perth, WA, 6009, Australia (VSK, ZW, SIH, ARH, MDG, TS); Developmental Biology Group, AgResearch Ltd, Hamilton, New Zealand (CDM); Experimental and Regenerative Neurosciences, School of Animal Biology, The University of Western Australia, Perth, WA, 6009, Australia (MF); Western Australian Neuroscience Research Institute, Perth, WA, 6009 (ARH, SIH); Centre for Cell Therapy and Regenerative Medicine, School of Medicine and Pharmacology, The University of Western Australia and Harry Perkins Institute of Medical Research, Perth, WA, 6009, Australia (ZW).

***Send correspondence to**: Miranda D. Grounds, PhD, School of Anatomy, Physiology and Human Biology, The University of Western Australia, Perth, WA, 6009, Australia; email: miranda.grounds@uwa.edu.au*

Acknowledgements.

This research was made possible by funding from The University of Western Australia (UWA: for MDG), and an International Postgraduate Scholarship and a Postgraduate Scholarship for International Tuition Fees from UWA (for VSK). MF is supported by an NHMRC Career Development Fellowship. ZW was supported by postgraduate research scholarships from UWA and the Centre for Cell Therapy and Regenerative Medicine Top-up Scholarship, School of Medicine and Pharmacology, UWA and Harry Perkins Institute of Medical Research, Perth, Western Australia.

***Disclosure statement**: The authors declare no conflicts of interest*

Author contributions:

Conception and design of research (VK, CM, TS, AH, MG); maintenance and monitoring of old male mice (CM, ZW); sampling of mice (VK, ZW, CM,TS, SH); experimental analyses of all nerve tissue (VK); data analysis and interpretation of experimental results (VK, CM, SH, MF, TS, AH, MG); preparation of figures (VK, TS, AH, MG); initial drafting of manuscript (VK, TS, AH, SH, MG); comments and approval of final version of the manuscript (all authors).

ABSTRACT

This study quantified morphological and molecular changes within sciatic nerves of aging male and female C57BL/6J mice aged between 3 and 27 months, analyzed using immunoblotting, immunohistochemistry and electron microscopy. In nerves of male mice aged 4, 15, 18, 22 and 24 months, protein analyses by immunoblotting showed significantly increased levels of heavy chain neurofilaments (SMI-32), vimentin, tau5, choline acetyltransferase (ChAT) and p62 by 18-22 months. Similar protein increases were seen in 26 month compared with 3 month old female mice. Immunostaining of longitudinal sections of old (27 month) male sciatic nerves revealed intense staining for tau5 and p62 that was increased compared to 3 months, but there were decreased numbers of axon profiles stained for ChAT or isolectinB4 (IB4) (motor and sensory axons respectively). Ultrastructural analysis revealed electron dense aggregates within axons in peripheral nerves obtained from old male mice; the proportion of axons that contained aggregates more than doubled between 15 and 27 months. Overall, the observed age-related accumulation of many proteins from about 18 months of age on wards suggests impaired mechanisms for axonal transport and protein turnover. These peripheral nerve changes may contribute to the morphological and functional muscle deficits associated with sarcopenia.

Keywords: Aging, axonal proteins, peripheral nerve, autophagy, protein aggregation, sarcopenia.

1. INTRODUCTION

In humans, the transition from mature adults to old age is associated with a significant decline in neuromuscular function and loss of skeletal muscle mass and strength (1-3)a condition known as sarcopenia (4, 5). The incidence of sarcopenia is reported to be about 14% by 65-69 years of age and may reach greater than 50% by 80 years (6). To date, most human muscle related aging studies have focused on analyzing changes in muscle mass and strength (1, 2, 6-8).

Given that motor afferent supply is essential for muscle health, contraction and function, surprisingly little is known about how this neurogenic component affects, or is influenced by, muscle aging (9-11). Loss of innervation at the neuromuscular junction (NMJ) has been described in aging humans (12, 13) and rodents (14-17) and is considered to be a major contributor to age-related functional, morphological and molecular changes in skeletal muscles. However it is not known whether myofiber denervation is related to deleterious changes in muscle cells or neurons, or both. Age-related changes in Schwann cell phenotype and plasticity may also be another contributing factor (18) .

Mice and rats are widely used as mammalian models for sarcopenia and are especially useful for time course studies to define the sequence of cellular and molecular changes during the earlier stages of sarcopenia (15, 19, 20). The value of multiple time points is emphasized to identify the earliest age-related changes, and their patterns of progression throughout life (21). Such studies are very difficult to reproduce in humans, given issues of sampling and the fact that humans age over a 20-30 year span whereas mice have a life expectancy of approximately 2.5 years. In aging female C57BL/6J mice we have previously

shown that loss of muscle mass is evident by 24 months (19, 22) and is associated with loss of innervation at the NMJ, although motor neuron numbers remain constant in the ventral horn (14). A comprehensive molecular analyses of mouse muscles across five ages (3, 15, 24, 27 and 29 months) found many changes at the mRNA and protein level that were associated with myofibre denervation(19).

The present study focuses on a quantitative analysis of age related molecular and morphological changes in the sciatic nerve of male C57BL/6J mice assessing multiple time points, ranging from 3 to 27 months of age. Longitudinal frozen sections of sciatic nerves were subjected to immunostaining for protein distribution; immunoblotting was used to quantify protein levels, and transmission electron microscopy (TEM) of transverse sections provided ultrastructural morphological analysis. In addition, we compared two extreme ages (3 and 26 months) in female C57BL/6J mice, to determine the impact of gender on age related changes in peripheral nerves.

2. MATERIALS AND METHODS

2.1 Mice and tissue collection

All animal experiments were conducted in accordance with the guidelines of the Ruakura Animals Ethics Committee, AgResearch Ltd Hamilton, New Zealand and the National Health and Medical Research Council of Australia and approved by the Animal Ethics Committee at The University of Western Australia (UWA). All animals were housed in standard animal cages and were maintained at a 12 hour light: dark cycle (lights turned on at 0700 hours and off at 1900 hours for animals at UWA, while for animals in New Zealand, lights turned on at 0600 hours and off at 1800 hours) with free access to meat free rat and mouse diet (protein,

20%; total fat, 4.8%; total fiber, 28.8%; total carbohydrate, 59.4%) fortified with vitamins and minerals (Specialty Feeds, Australia) and drinking water.

C57BL/6J male mice aged 4, 15, 18, 22 and 24 months were from a mouse breeding facility at AgResearch Ltd, New Zealand (NZ). These mice were killed by $C0_2$ inhalation followed by cervical dislocation. Female C57BL/6J mice aged 3 and 26 months were obtained from the Animal Resource Centre in Western Australia and these were killed by cervical dislocation while under terminal anesthesia (2% Attane isoflurane, Bomac, NSW, Australia, 400mL NO_2 and 1.5L O_2) due to differing animal ethics requirements. Sciatic nerves from these male and female mice were dissected at the gluteal level, carefully cleaned from muscle tissue and snap frozen in liquid nitrogen for protein analysis.

Additional cohorts of male C57BL/6J mice aged 3, 15 and 27 months were obtained from the Animal Resource Centre, Western Australia. Sciatic nerves from these mice were fixed and processed for TEM and immune fluorescence studies. A 1mm length of the distal end of the sciatic nerve adjacent to the muscle was dissected and immediately fixed in 2.5% (w/v) glutaraldehyde (Sigma, Australia # G-7776) for ultrastructural studies using TEM and the rest of the nerve was fixed in 4% (w/v) paraformaldehyde (Sigma, Australia #P6148) for immunofluorescence studies (Fig. 1).

2.2 Immunohistochemical staining of cryosections of sciatic nerve

Freshly collected sciatic nerves were gently straightened and attached to a wooden spatula, fixed in 4% (w/v) paraformaldehyde and cryoprotected in 30% (w/v) sucrose solution in PBS for 24 hours at 4^{o}C (Fig. 1). Nerves were removed from the wooden spatula and embedded

in tissue freezing medium (Leica, Australia), snap frozen in isopentane cooled in dry-ice and stored at -80^{0}C. Frozen blocks with embedded nerves were sectioned longitudinally at 16µm thickness using a Leica CM3050 cryostat, and frozen sections were collected onto gelatin coated slides, and stored at -20^{0}C until further processing. Frozen longitudinal nerve sections were stained with several different antibodies (Table 1). Sections were rinsed with PBS for five minutes three times, blocked for one hour in antibody diluent, consisting of PBS with 10% (v/v) normal horse serum and 0.2% (v/v) Triton X-100, and incubated overnight in primary antibodies at 4^{o}C. BEAT ^{TM} blocking solution (Invitrogen #50-300) was used to minimize non-specific interaction between anti-mouse secondary antibodies andendogenous Ig in mouse PN tissue. After washing again in PBS and exposure to appropriate secondary antibodies (Table 2), sections were covered with fluorescence compatible mounting medium (DAKO-S3023, USA) and cover-slipped (23).For choline acetyltransferase (ChAT) immunolabeling, an additional step of antigen retrieval was added in the beginning, which involveda 10 minute wash with 0.1% Triton-X100 and 0.01mg/ml proteinase k in PBS and overnight incubation at 55°C in 50% formamide. This procedure enhances antibody penetration and optimises visualisation of ChAT (24, 25).Stained sections were observed and photographed using a Nikon eclipse E-400 fluorescent microscope.

2.3 Quantification of immunostained axons in longitudinal nerve sections

The number of positively labelled axons in each sciatic nerve was quantified from longitudinal sections immunostained for heavy chain neurofilament (SMI-32), β-IIItubulin (TuJ1), ChAT or isolectin B4 (IB4).Three longitudinal sections per nerve were viewed using a Nikon Eclipse E400 microscope and photographed at 20x magnification along the length of the section from the proximal to the distal end. The sections were selected from across the

width of the nerve to provide a representative sample of the nerve cross section. The numbers of stained axons crossing arbitrarily placed lines located at the proximal, middle and distal parts of each nerve were counted and averaged; the nerve width at these sites was also measured to establish the number of axons per nerve width (Fig. 2A).

2.4 Protein extraction and immunoblotting

Immunoblotting was performed using a number of different antibodies (Table 1). Snap frozen sciatic nerves were homogenized with a Polytron homogenizer in buffer containing 20mM HEPES (Life technologies, USA) and 4% (w/v) sodium dodecyl sulphate (SDS) (Promega, USA,) supplemented with protease and phosphatase inhibitor tablets (Roche, Mannheim, Germany), followed by sonication for 10 seconds using a Vibra Cell ultrasonic processor at 40% amplitude (Vibra Cell Sonics & Materials Inc, #VCX 130) (26). The tissue suspension was centrifuged at 19,600g for 10 min which did not leave any pellet detectable by visual examination. After centrifugation the concentration of protein in the supernatant was quantified with the *DC*™ protein assay (Bio-Rad, NSW, Australia). Samples of protein (7µg/well) were resolved on 4-15% SDS-PAGE TGX gels (Bio-Rad, NSW, Australia, #465-1086) and transferred onto 0.2µm pore size nitrocellulose membrane (Bio-Rad, NSW, Australia, #170-4158) using a Trans Turbo Blot system (Bio-Rad, NSW, Australia). A common protein sample was loaded on each gel to normalize for detection efficiencies across membranes. After transfer, membranes were stained with Ponceau S red stain (Sigma P3504, Australia) to visualize the total protein, which was used as a loading control (27, 28). Studies have shown that total protein is a more reliable loading control than commonly used housekeeping proteins (27, 29-31) which can change with ageing. A combined intensity of all

bands in a single lane was used to normalize the test protein band intensities. All primary antibodies were diluted in 5% (w/v) BSA in 1% (v/v) TBS-T buffer. Horseradish peroxidase (HRP) conjugated secondary antibodies were from Thermo Fischer Scientific, MA, USA (Table 3). Blots were developed using Perkin Elmer Western Lightening Ultra (#NEL111001EA) and the chemiluminescent signal was captured using a ChemiDoc MP Imaging System (Bio-Rad, NSW, Australia). Resultant images were quantified using ImageJ software by normalizing bands to the respective total protein stained with Ponceau S red stain in the same gel (Supplementary Fig.1). All immunoblot images in the figures represent samples immunoblotted on to the same membrane.

2.5 Transmission electron microscopy (TEM)

TEM was used to monitor age related ultrastructural changes in nerves of C57BL/6J male mice from 3 age groups (3, 15 and 27 months). A 1mm length of distal sciatic nerve was fixed in fixative buffer containing 2.5% (v/v) glutaraldehyde (Sigma-G7776) and 2% (w/v) paraformaldehyde (Sigma-P6148) in 0.13M Sorenson's buffer with 2% (w/v) sucrose at pH 7.2. This was post fixed in 1% (v/v) osmium tetroxide (ProScitech, Queensland, Australia) for 60 minutes while shaken. The tissue was then dehydrated through ethanol series to propylene oxide, infiltrated, and processed into an Araldite Procure mixture (ProScitech), using a Lynx processor. Transverse sections were collected using a diamond knife and collected onto copper grids and stained with 2.6% (w/v) lead citrate. High magnification (16000x) images were digitally generated using TEM (JEOL 2100; Jeol, Tokyo, Japan) with a 11-Megapixel digital camera (Orius; Pleasanton, CA).

2.6 Statistical Analysis

The number of immunostained axons from 3 and 27 month old nerves was compared using a two-tailed unpaired T-test. Protein quantification data obtained by immunoblotting from C57BL/6J males were analyzed using one-way ANOVA followed by Fischer's Least Significant Difference (LSD) tests for direct comparisons between individual means. For females, protein quantification data obtained by immunoblotting were compared using two-tailed unpaired T-test. Statistical analysis of the percentage of axons with aggregates was conducted using one way ANOVA followed by Fischer's Least Significant Difference (LSD) tests. For all statistical analyses significance threshold was set at $P \leq 0.05$.

3. RESULTS

3.1 Quantification of immunostained axons in longitudinal nerve sections

Longitudinal sciatic nerve sections from C57BL/6J males aged 3 or 27 months were immunostained to enable quantification of motor (ChAT) and sensory (IB4) axons and to examine the distribution and localization of cytoskeletal proteins (heavy chain neurofilaments-SMI-32 and tubulin). There was a significant age related decrease in the number of immunostained axons visualized per unit width of nerve for axons immunoreactive for ChAT (motor) or IB4 (nociceptive sensory) (Fig. 2B-E). Small bundles of axons immunopositive for IB4 were seen in both young and aged nerves. Similar bundles were not seen in sections stained for ChAT. On average there were 4-5 IB4 labelled axon bundles per nerve, a number that was not altered with age. These bundles generally contained 3-5 axons. Immunoreactivity was sometimes discontinuous in old nerves (Fig. 2C)

suggesting loss of protein integrity, rather than loss of entire axons. There was no significant change in the number of axons immunoreactive for SMI-32 (Fig. 2F) or β-III tubulin (Fig. 2G).

3.2 Quantification of cytoskeletal proteins in sciatic nerves - immunoblotting

Neurofilaments and microtubules are essential components of the cytoskeleton necessary to maintain neuronal structure and function, including anterograde and retrograde transport systems (32, 33). Pathological accumulation of neurofilaments is harmful to neurons and is seen in numerous neurological diseases (33). Immunoblotting was used to quantify levels of heavy neurofilaments (SMI-32), vimentin, β-III tubulin, α-tubulin and the microtubule-associated protein tau in sciatic nerves of male and female C57BL/6J mice.

3.2.1 SMI-32

Intermediate filaments provide for the structural support and diameter maintenance of axons, the latter influencing the speed of nerve impulse conduction. SMI-32 antibody recognizes a non-phosphorylated epitope of heavy neurofilaments subunits which are particularly needed in larger neurons with highly myelinated, fast conducting axons (34). In C57BL/6J males, the amount of SMI-32 neurofilament protein increased with age (Fig. 3A, D), with levels significantly higher at 18, 22 and 24 months compared with 4 months ($P \leq 0.05$). In females, SMI-32 levels tended to increase with age ($P=0.08$) (Fig. 3F, I).

3.2.2 Vimentin

Vimentin is an intermediate filament abundantly expressed in a wide variety of cell types including Schwann cells, neuronsand fibroblasts. In the peripheral nervous system (PNS) this intermediate filament negatively regulates myelination, and expression is upregulated in Schwann cells and neurons during nerve regeneration (35). Vimentin protein levels increased with age in sciatic nerves of male and female C57BL/6J mice. In male mice, vimentin protein levels were significantly higher at 18 and 22 months compared with 4 and 15 months (Fig.3B, E). Levels declined at 24 months of age, although remained significantly elevated compared with 4 and 15 months. In females, vimentin levels were significantly higher at 26 months compared with 3 months (Fig. 3G, J).

3.2.3 β-III tubulin and α-tubulin

Microtubules are assembled from dimers of β and α-tubulin. These tubulin isoforms are expressed in a wide range of cell-types including neurons of both the central nervous system (CNS) and PNS (36-38). β-III tubulin and α-tubulin protein levels remained unchanged in nerves across all age groups in both males (Supplementary Fig.2A-E) and females (Supplementary Fig.2F-J), supporting the assessments of numbers of β-III tubulin immunopositive axons (Fig. 2G).

3.3 Tau protein levels in sciatic nerves

The microtubule associated protein tau plays a major role in maintaining the normal morphology of neurons and promoting microtubule assembly and stabilization (39, 40). Abnormal phosphorylation and aggregation of tau has been implicated in several

neurodegenerative disorders of the CNS (41). We observed age-related increases in tau protein levels in both male and female sciatic nerves. In males, tau protein levels were significantly higher at 22 and 24 months compared with 4 and 15 months (Fig. 4A, C). Female 26 month old nerves also had higher tau levels compared with nerves at 3 months (Fig. 4E, G). In addition, qualitative immunostaining for tau protein in longitudinal sections of male young and old sciatic nerves confirmed a marked increase in immunoreactivity for tau protein at 27 month, compared with 3 month (Fig. 4D).

3.4 Protein quantification for S100β and ChAT

3.4.1 S100β protein

Schwann cells myelinate peripheral axons, provide trophic support and can modulate synaptic activity at the NMJ (42-44). We previously described an apparent deterioration of Schwann cells that ensheath peripheral nerve terminals in 29 month old female C57BL/6J mice using S100β to visualize Schwann cells(14). In the present study, immunoblotting was used to quantify levels of S100β protein in male and female sciatic nerves. In male nerves (Fig. 5A, D) S100β protein tended to increase with age (P=0.16), however there was a high variability within age groups. S100β protein was significantly increased in 26 month female nerves, compared with nerves at 3 months (Fig. 5F, I).

3.4.2 Choline acetyltransferase (ChAT)

ChAT is the enzyme responsible for the biosynthesis of acetylcholine, the neurotransmitter at the NMJ (45). ChAT is presently the most specific indicator for monitoring the functional state of cholinergic neurons in CNS and PNS (46, 47). Defects in the cholinergic system have been documented in aging and neurodegeneration (48). In male sciatic nerves (Fig. 5B, E),

ChAT levels increased between 15 and 18 months and remained elevated at 22 and 24 months compared with younger ages (3 and 15 months). A similar age-related increase was seen in female sciatic nerves (Fig. 5G, J). Note that this increase in protein was seen even though immunohistochemistry revealed fewer ChAT immunopositive axons (Fig. 2B, D).

3.5 Markers of autophagy (p62, LC3B, LAMP1)

Increased levels of key proteins with age (SMI-32-heavy neurofilament, vimentin, tau and ChAT) suggested accumulation of these proteins, possibly due to dysfunctional protein degradation machinery in old nerves. The autophagic/lysososmal system and ubiqutin/proteasome system are two major catabolic pathways that degrade proteins and organelles in the cell. Because accumulation of proteins may reflect an imbalance between the rates of protein damage and protein turnover (49, 50), we quantified autophagy markers p62, LC3B and lysosomal marker LAMP1 in young and old nerves.

3.5.1 p62/ Sequestosome 1

p62 acts as a receptor that binds and delivers polyubiquitinated proteins to the autophagy machinery to enable their degradation in the lysosome (51). In male nerves, levels of p62 increased with age and were significantly higher at 22 and 24 months compared with 4 and 15 months (Fig. 6A, C). A striking increase of p62 with age was also evident in females (Fig.6E, G). Immunohistochemical localization of p62 in longitudinal sections of male nerves aged 3 and 27 months confirmed increasedp62 protein with age (Fig. 6D).

3.5.2 LC3

During the formation of autophagosome, the microtubule associated protein 1 light chain-3 (LC3I) converts to LC3II by lipidation. At the autophagosome, LC3II plays an important role in

selecting the cargo for degradation by binding to p62/SQSTM1 protein aggregates (52). Therefore the level of LC3II (LC3II/LC3I+LC3II ratio) is used to evaluate autophagy (53, 54). The ratio of LC3II to total LC3(I+II) was unchanged with age in both males (Supplementary Fig. 3C) and females (Supplementary Fig. 3H), however there were gender specific differences in the relative intensities of LC3I and LC3II bands. In males (Supplementary Fig.3A) the LC3I band was more prominent than LC3II at all ages, whereas in females (Supplementary Fig. 3F) both bands were equally prominent, although the intensity was higher in old compared with young nerves. In addition, we quantified levels of LC3I and II relative to total protein in males and females. The levels of LC3I in males increased with age and were significantly higher at 15, 18 and 24 months compared with 4 months (Supplementary Fig.3D). The levels of LC3II remained unchanged at all ages (Supplementary Fig. 3E). LC3I and II levels were higher in old female nerves compared with young (Supplementary Fig. 3I, J).

3.5.3 LAMP1

Lysosomal associated membrane proteins LAMP1 and LAMP2 are lysosomal transmembrane proteins with considerable sequence homology; they maintain lysosomal stability and integrity (55, 56). Due to their sequence homology the LAMP proteins have overlapping functions, and both LAMP1 and LAMP2 are essential for phagosome-lysosome fusion. Loss of both LAMPs markedly inhibits phagosome maturation (57). In our study, LAMP1 protein levels varied in nerves of male mice aged either 4, 15, 18, 22 or 24 months, but due to high variance the differences were not significant (Supplementary Fig. 4A, C). However, LAMP1 levels were increased in 26 month old female nerves compared with 3 month nerves (Supplementary Fig.4D, F).

3.6 Intra-axonal aggregates in old nerves - ultrastructure

Intracellular protein aggregates are a common feature of numerous disorders of the CNS and PNS and can be readily visualized using TEM (52, 58-60). Transverse ultrathin sections of sciatic nerve from male mice aged 3, 15 or 27 months were examined for the presence of aggregate macromolecules. All of the axons in the nerves were viewed and the percentage of axons that contained aggregates determined and expressed as the number of aggregates/total number of axons x100. Aggregates were not evident at 3 months (Fig. 7A, B). At 15 months aggregates were observed in 0.38±0.1% of examined axons, and at 27 months there was a significant increase compared to 3 months, with aggregates present in 0.82±0.2%of axons (Fig. 7E).We did not observe any obvious aggregates within Schwann cells of old nerves, howeverthis might be due in part to the relatively small amount of cytoplasm visible for Schwann cells in many of the EM sections.

4. DISCUSSION

This comprehensive time-course study of aging sciatic nerves from male and female C57BL/6J mice, from 3 to 27 months, describes significant molecular and morphological changes, some evident as early as 18 months. In old nerves there was a decrease in the number of IB4 positive nociceptive axons and ChAT positive motor axons. Immunoblots of male nerves at 18-22 months revealed significantly increased levels of heavy chain neurofilaments (SMI-32), tau, ChAT and vimentin, as well as an increase in the autophagy marker p62 relative to total protein in the nerves. Similar age-related protein increases were seen in nerves of 26 month old female mice, including an increase in S100B protein levels. Using EM we observed intra-axonal protein aggregation in axons in old nerves. These various observations are consistent with altered axon transport efficiency and implicate

alterations in protein turnover as possible mechanisms for age-related accumulation of intra-axonal proteins. The consequences of these changes in aging nerves and their possible relevance to sarcopenia are discussed below.

4.1 Accumulation of cytoskeletal proteins in aging nerves

Function of the PNS is significantly affected by aging (61), with morphological changes detectable both within the cell bodies of neurons, their axons and accompanying Schwann cells. There is segmental demyelination, myelin thinning, axonal degeneration, Schwann cell proliferation and axonal swelling (62), as well as accumulation of mis-folded and damaged proteins (63). Within parent cell bodies the accumulation of damaged organelles, proteins and lipids is presumed to be related to an age-related decrease in efficiency of protein degradation mechanisms, associated with several peripheral neuropathies and less effective neurotransmission (64, 65). Our study on aging murine sciatic nerves confirms and extends knowledge of altered protein turnover in aged peripheral nerves, and strongly suggestsa dysfunctional transport system and inefficient protein degradation machinery.

It is emphasized that both the retrograde and anterograde transport systems are of key importance for NMJ function, due to the great distance from the cell body and the intervening length of axons in peripheral nerves. In old nerves, total levels of heavy neurofilament protein (an important cytoskeletal component) quantified by immunoblotting were increased, although tubulin levels did not significantly change with age. Altered expression of cytoskeletal proteins has been implicated in demyelinating diseases and peripheral neuropathies (66) and accumulation of neurofilaments as well as defects in axonal transport have also been implicated in neurodegenerative disease in the

PNS (67, 68) and CNS (69, 70).Phosphorylation regulates important aspects of neurofilament transport and function. While a key pathological hallmark of several neurodegenerative diseases is abnormal phosphorylation and accumulation of neurofilaments (33, 71) the antibody used in our study specifically did not bind to phosphorylated neurofilaments and thus we have no information on this aspect. Studies in mouse models of spinal muscular atrophy show aberrant cytoskeletal organization in 60% of NMJs, accompanied by an accumulation of phosphorylated and non-phosphorylated forms of medium and heavy chain neurofilaments,associated with motor deterioration and muscle atrophy (69). Our study implies that increased amounts of heavy neurofilament in nerves are also observed in normal aging.

4.2 Age related changes in tau protein levels

Tau is a microtubule associated protein that plays a major role in promoting microtubule assembly and stabilization (39, 40). Abnormal phosphorylation and aggregation of tau has been implicated in neurodegenerative CNS disorders (72). One study in humans measured the levels of phosphorylated and total tau in sciatic nerves for humans aged 60-91 years and reported increased phosphorylation (without a change in the total abundance of tau) in older ages (90-91), compared with younger ages (60-68years) (73).To our knowledge, our longitudinal study in mice is the first to report changes in the abundance of tau protein in aging peripheral nerves, withtau5 protein significantly elevated in males at 22 and 24 months, and in females aged 26 months.

Disequilibrium between tau phosphorylation and de-phosphorylation destabilizes the axonal cytoskeleton, reduces tau's affinity for microtubules and promotes self-association of tau

and formation of neurofibrillary tangles (74).These tangles are often a prime cause of synaptic and neuronal degeneration (75, 76). Thus the dramatic increase in tau in old sciatic nerves may affect axon transport, contribute to NMJ dysfunction, and perhaps compromise muscle contraction. Interestingly, synaptic accumulation of hyper-phosphorylated tau is associated with dysfunction of the ubiquitin proteasome pathway (UPP) (77). Normally tau degradation takes place through the UPP; the p62 protein interacts with polyubiquitinated tau through its ubiquitin binding domain and facilitates its proteasomal degradation (78). Accumulation of p62 in neurofibrillary tangles and its co-localization with hyper-phosphorylated tau raises the possibility that the inability of p62 to shuttle polyubiquinated tau, contributes to tau accumulation (78-80). Our study shows an age-related increase in p62 protein levels in old nerves, thus our increasedtau protein may also reflect the impact of elevated p62 on normal tau processing (see also 4.5).

4.3 ChAT accumulation, impairment in axonal transport

The transport of molecules and organelles up and down an axon is fundamental for the maintenance of neuronal homeostasis and the health of cells and their targets (81). ChAT is an enzyme which catalyzes the synthesis of the neurotransmitter acetylcholine that is crucial for signaling across the NMJ. ChAT is synthesized in the neuronal cell body and transported anterogradely to the nerve terminal (82-84). While we show a significant decrease in the incidence of ChAT immunostained axons in old nerves, this might reflect an altered pattern of uniform immunostaining, rather than loss of axons *per se*. Indeed, immunoblotting revealed that total ChAT protein levels increased within old nerves by 18 months.

This apparent anomaly might also be explained in part by the extent of heterogeneous myofibre denervation during sarcopenia, where many NMJs become partially and then fully denervated (14, 19) between 19 and 25 months (15, 17). The axons that have lost their NMJ target may then accumulate ChAT protein due to reduced utilization of this synthesizing enzyme at the NMJs. Others have reported that ChAT activity in the EDL and soleus muscle is reduced by almost 40% in old rats (85, 86).

4.4 Altered Schwann cell phenotype

In addition to changes in axons there are age-related changes in Schwann cell phenotype (18, 87, 88). Age-related changes in inflammatory/immune responses and altered processing of lipids are thought to be related to diminished Schwann cell function (87). Aged Schwann cells are also less capable of supporting axonal regeneration after injury (18). We observed accumulation of vimentin and S100B in old sciatic nerves that peaked at about 2 years, providing evidence for altered Schwann cell phenotype in old nerves. S100B secreted or released from glia at high concentrations can be pathogenic and have pro-inflammatory effects(89) and S100B can also bind with tubulins and tau, potentially affecting axonal function. Altered processing of vimentin has been reported to have adverse effects on peripheral myelin and axonal stability (90), but since vimentin is also expressed in fibroblasts as well as Schwann cells, the observed increase in vimentin levels in old nerves is not easy to intepret. In aged human sural nerves there are changes not only in axons and myelin but also thickening of vascular basement membranes and the perineurial sheaths(91) , perhaps indicating additional changes in fibroblast number or function. .

4.5 Protein degradation pathways and neuronal function

The unique morphology of neurons and the plasticity of synapses impose special challenges on the cellular machinery for both protein synthesis and degradation (92). Protein aggregates resulting from perturbations in protein degradation pathways are neuropathological events found in a number of seemingly unrelated neurodegenerative diseases (93, 94). EM identified intra-axonal inclusions, presumably proteinaceous in nature, in aged murine axons.

Autophagy and ubiquitin proteasome pathway (UPP) are two main protein degradation pathways in mammalian cells (95-98) and it is suggested that the function of these pathways is altered in aging (49, 99-102), resulting in accumulation of misfolded and aggregate-prone toxic proteins. We observed an abundance of p62 protein in aged nerves from both male and female mice, which mayindicate altered function of autophagy and UPP (103-105). Accumulation of protein aggregates that are associated with p62 is a characteristic of several neurodegenerative disorders, including Alzheimer's, Parkinson's and Huntington's disease(106).

Although accumulation of p62 with ubiquitin containing aggregates is largely viewed as a hallmark of impaired autophagy (104, 105), some studies suggest that p62 has a protective role and mediates degradation of aggregated proteins (78, 107) e.g. in Alzheimer diseases, p62 shuttles polyubiquitinated tau to the proteasome for degradation (78).Thus elevated p62 in the sciatic nerves of old mice may have a compensatory function to target aggregated proteins.

To further interrogate the possibility of perturbed autophagy in aged murine nerves, we measured amounts of LC3-I and II and LAMP1. Conversion of LC3-I into LC3-II is used to monitor autophagy, although interpretation of the results is not straightforward (54). LC3-II itself is degraded by autophagy and accumulation of LC3-II along with accumulation of LAMP proteins is seen in cases where autophagy is impaired (108). Age-related changes in LC3and LAMP1 protein amounts were more pronounced in female compared with males, pointing to gender specific differences. In aged female nerves, amounts of both LC3-I and LC3-II in combination with LAMP1 were increased, suggesting an altered autophagy pathway.

4.6 Relationship between time course of peripheral nerve changes and sarcopenia

How does the timing of these peripheral nerve changes relate to sarcopenia in mice? We previously demonstrated age-related loss of mass in quadriceps muscles of female C57BL/6J mice aged 24 months (19, 22) and some but not all limb muscles of male FVB mice aged 28 months (109).This 2014 study in FVB mice also documented the progressive age-related reduction involuntary wheel running capacity (measured monthly between 6 and 28 months), with decreased speed and distance pronounced from about 18 months of age. Such decreased exercise performance may be partly due to deterioration of muscle function (among other age-related physiological changes). An altered circadian pattern of running by old mice, in addition to less distance run, is also well documented (110).

Time course studies are very informative and parallel analyses of muscles from the same aging male C57BL/6J mice, that provided the sciatic nerves for the present study, showed evidence of sarcopenia by 18 months (White et al, manuscript submitted).In brief, the standardized (to tibia length) mass of quadriceps was the most affected with a significant

9% decrease between 4 months and 18-22 months and a further reduction of mass, 16%, between 22 and 24 months (P≤0.05).The mass of the gastrocnemius, soleus and tibialis anterior (TA) muscles decreased significantly between 4 and 24 months, by 23%, 19% and 10% respectively (P≤0.05).. Gastrocnemius, soleus and TA muscles are innervated by the sciatic nerve, while the femoral nerve innervates quadriceps muscles. The question of whether sarcopenia is primarily driven by early changes within nerves, or within muscles, remains unresolved by this time course study. However we can conclude that, at least in male C57BL/6J mice,age-related molecular alterations in sciatic nerves occurred *before* loss of mass in muscles innervated exclusively by this nerve. These neuronal changes may be contributing to diminished muscle function, which may precede loss of muscle mass (2). We did not evaluate muscle function in our mouse cohorts.

A time course study (15) of stained NMJ visualized on TA muscles of aging female C57BL/6J mice (at 6 ages), concluded that changes in the (muscle) post-synaptic NMJ were evident by 19 months, followed by loss of pre-synaptic nerves that was pronounced by 25 months. While these data support changes first manifesting at the muscle surface, they do not exclude the possibility that molecular changes within the axons (such as we describe) may have dictated this altered NMJ morphology. The relative role of the nervous system and of myofibres in sarcopenia is discussed in a recent review (111) and has been addressed experimentally using a mouse model where sarcopenia was accelerated by loss of the anti-oxidant CuZn-superoxide dismutase (CuZnSOD) in mice, combined with selective modulation of levels of CuZnSOD in muscles and nerves (112). The latest paper in this series targeted deletion of CuZnSOD specifically to neurons (nSod1KO mice) and concluded that deficits in

both tissues are required to recapitulate the loss of muscle observed in Sod1KO mice (113). The challenge of this conundrum remains.

5. CONCLUSIONS

The progression of sarcopenia is an increasingly important clinical problem and the neurogenic perspective is crucial. A striking finding of our longitudinal study of sciatic nerves from aging C57BL/6J mice was the increasing accumulation of many proteins related to cytoskeletal and proteolytic functions, suggestive of age-related impaired axonal transport and dysfunction of degradation mechanisms. These neuronal alterations, combined with increasing intra-axonal protein aggregates, could progressively impair axonal transport, excitability, the supply of neurotransmitter and other trophic molecules to NMJs, thereby reducing synaptic efficacy and muscle contractility. This is a plausible explanation that deserves further testing.

Acknowledgements

We thank Michael Archer for technical assistance with electron microscopy and the Australian Microscopy and Microanalysis Research Facility at the Centre for Microscopy, Characterization and Analysis, UWA. We also thank Dr. Hannah Crabb of Curtin University for help with collecting sciatic nerves from the female C57BL/6J mice.

FIGURE LEGENDS

Figure 1. Image of a dissected sciatic nerve and schematic representation showing processing of thenerve and collection of cryosections.

Figure 2. Quantification of immuno-labelled axons in longitudinal sections (16µm thickness) of 3 and 27 month old male C57BL/6J mouse sciatic nerves. Schematic representation of axon counting from longitudinal sections(LS) of nerve: (A)the yellow lines represent arbitrarily placed lines located at the proximal, middle and distal part of the nerve.Representative images of LS of nerveslabelled with antibodies recognising ChAT (B) and isolectinB4 (IB4) (C).Quantification of the axon numbers (per 500µm of nerve section width)positively labelled for ChAT (D), IB4 (E), SMI-32 (F) or β-III tubulin (G). Axon numbers are expressed as mean±SEM.N= 5-7 mice per group., ***P≤0.001.

Figure 3. Quantification of SMI-32 and vimentin protein in sciatic nerves fromC57BL/6J males and females detected by immunoblotting. SMI-32 (A, D, F, I) and vimentin (B,E,G,J) proteins were quantified in males aged 4-24 months (A-E) and females aged 3 and 26 months (F-J). Per each age group, N=4-8 mice were used for males and N=7 mice were used for females. Bands immuno-reactive toSMI-32 and vimentin antibodies were normalized to total protein per respective lane visualized with Ponceau S red (C, H). Data (D, E, I, J) are mean ± SEM. *P≤0.05, **P≤0.01, ***P≤0.001 (ANOVA with Fisher's LSD tests). Y axis represents arbitrary units.

Figure 4. Quantification of Tau5 protein in sciatic nerves fromC57BL/6J mice detected by immunoblotting (males and females) and immunohistochemistry (males). Tau5 protein was

quantified by immunoblotting in males aged 4-24 months (A-C) and females aged 3 and 26 months (E-G). Per each age group, N=4-8 mice were used for males and N=7 mice were used for females. Bands immuno-reactive to tau5 antibody were normalized to total protein per respective lane visualized with Ponceau S red (B,F). Data (C, G) are mean ± SEM. * P≤0.05, **P≤0.01, ***P≤0.001 (ANOVA with Fisher's LSD tests). Y axis represents arbitrary units. Longitudinal sciatic nerve sections from 3 and 27 month old male C57BL/6J mice immunolabelled with Tau5 antibody (D).

Figure 5. Quantification of S100 and ChAT protein in sciatic nerves from C57BL/6J males and females detected by immunoblotting. S100 (A, D, F, I) and ChAT (B, E, G, J) proteins were quantified in males aged 4-24 months (A-E) and females aged 3 and 26 months (F-J). Per each age group, N=4-8 mice were used for males and N=7 mice were used for females. Bands immuno-reactive to S100 and ChAT antibodies were normalized to total protein per respective lane visualized with Ponceau S red (C, H). Data (D, E, I, J) are mean ± SEM.* P≤0.05, **P≤0.01, ***P≤0.001 (ANOVA with Fisher's LSD tests). Y axis represents arbitrary units.

Figure 6. Quantification of p62 protein in sciatic nerves from C57BL/6J males and females detected by immunoblotting. p62 protein was quantified by immunoblotting in males aged 4-24 (A-C) and females aged 3 and 26 months (E-G).Per each age group, N=4-8 mice were used for males and N=7 mice were used for females. Bands immunoreactive to p62wasnormalized to total protein per respective lane visualized with Ponceau S (B, F). Data (C, G) are mean ± SEM. * P≤0.05, **P≤0.01, ***P≤0.001 (ANOVA with Fisher's LSD

tests). Y axis represents arbitrary units. Longitudinal sciatic nerve sections from 3 and 27 month old male mice immunolabelled with p62 antibody (D).

Figure 7. TEM images of axons from 3 and 15 month old male C57BL/6J mice and quantification of axons with intra-axonal aggregates at 3, 15 and 27 months. Representative images of transverse (A, C) and longitudinal (B, D) sections from a 3 month old sciatic nerve (A-B) compared with a 15 month old nerve (C, D). Axons containing intra-axonal aggregates were quantified and data expressed as a percent of the total number of analysed axons (E). Data are mean ± SEM with N=4 per age group.* $P \leq 0.05$ relative to 3 months: Note that no aggregates were found at this age.

6. REFERENCES

1. Cruz-Jentoft AJ, Baeyens JP, Bauer JM, et al. Sarcopenia: European consensus on definition and diagnosis: Report of the European Working Group on Sarcopenia in Older People. Age Ageing 2010;39:412-23

2. Clark BC, Manini TM. Sarcopenia =/= dynapenia. J Gerontol A Biol Sci Med Sci 2008;63:829-34

3. Cederholm TE, Bauer JM, Boirie Y, et al. Toward a definition of sarcopenia. Clin Geriatr Med 2011;27:341-53

4. Rosenberg IH. Sarcopenia: origins and clinical relevance. Clin Geriatr Med 2011;27:337-9

5. Rosenberg IH. Sarcopenia: origins and clinical relevance. J Nutr 1997;127:990-1

6. Janssen I. Evolution of sarcopenia research. Appl Physiol Nutr Metab 2010;35:707-12

7. Denison HJ, Cooper C, Sayer AA, et al. Prevention and optimal management of sarcopenia: a review of combined exercise and nutrition interventions to improve muscle outcomes in older people. Clin Interv Aging 2015;10:859-69

8. Berger MJ, Doherty TJ. Sarcopenia: prevalence, mechanisms, and functional consequences. Interdiscip Top Gerontol 2010;37:94-114

9. Delbono O. Neural control of aging skeletal muscle. Aging Cell 2003;2:21-9

10. Kwan P. Sarcopenia, a neurogenic syndrome? J Aging Res 2013;2013:1-10

11. Kwan P. Sarcopenia: the gliogenic perspective. Mech Ageing Dev 2013;134:349-55

12. Aagaard P, Suetta C, Caserotti P, et al. Role of the nervous system in sarcopenia and muscle atrophy with aging: strength training as a countermeasure. Scand J Med Sci Sports 2010;20:49-64

13. Lexell J. Evidence for nervous system degeneration with advancing age. J Nutr 1997;127:1011S-3S

14. Chai RJ, Vukovic J, Dunlop S, et al. Striking denervation of neuromuscular junctions without lumbar motoneuron loss in geriatric mouse muscle. PLoS One 2011;6:1-11

15. Cheng A, Morsch M, Murata Y, et al. Sequence of age-associated changes to the mouse neuromuscular junction and the protective effects of voluntary exercise. PLoS One 2013;8:1-8

16. Li Y, Lee Y, Thompson WJ. Changes in aging mouse neuromuscular junctions are explained by degeneration and regeneration of muscle fiber segments at the synapse. J Neurosci 2011;31:14910-9

17. Valdez G, Tapia JC, Kang H, et al. Attenuation of age-related changes in mouse neuromuscular synapses by caloric restriction and exercise. Proc Natl Acad Sci U S A 2010;107:14863-8

18. Painter MW, Brosius Lutz A, Cheng YC, et al. Diminished Schwann cell repair responses underlie age-associated impaired axonal regeneration. Neuron 2014;83:331-43

19. Barns M, Gondro C, Tellam RL, et al. Molecular analyses provide insight into mechanisms underlying sarcopenia and myofibre denervation in old skeletal muscles of mice. Int J Biochem Cell Biol 2014;53:174-85

20. Ibebunjo C, Chick JM, Kendall T, et al. Genomic and proteomic profiling reveals reduced mitochondrial function and disruption of the neuromuscular junction driving rat sarcopenia. Mol Cell Biol 2013;33:194-212

21. Coleman P, Finch C, Joseph J. The need for multiple time points in aging studies. Neurobiol Aging 2004;25:3-4

22. Shavlakadze T, McGeachie J, Grounds MD. Delayed but excellent myogenic stem cell response of regenerating geriatric skeletal muscles in mice. Biogerontology 2010;11:363-76

23. Godinho MJ, Teh L, Pollett MA, et al. Immunohistochemical, ultrastructural and functional analysis of axonal regeneration through peripheral nerve grafts containing Schwann cells expressing BDNF, CNTF or NT3. PLoS One 2013;8:1-19

24. Shakhbazau A, Kawasoe J, Hoyng SA, et al. Early regenerative effects of NGF-transduced Schwann cells in peripheral nerve repair. Mol Cell Neurosci 2012;50:103-12

25. Eggers R, Tannemaat MR, Ehlert EM, et al. A spatio-temporal analysis of motoneuron survival, axonal regeneration and neurotrophic factor expression after lumbar ventral root avulsion and implantation. Exp Neurol 2010;223:207-20

26. Shavlakadze T, Soffe Z, Anwari T, et al. Short-term feed deprivation rapidly induces the protein degradation pathway in skeletal muscles of young mice. J Nutr 2013;143:403-9

27. Romero-Calvo I, Ocon B, Martinez-Moya P, et al. Reversible Ponceau staining as a loading control alternative to actin in Western blots. Anal Biochem 2010;401:318-20

28. White JP, Gao S, Puppa MJ, et al. Testosterone regulation of Akt/mTORC1/FoxO3a signaling in skeletal muscle. Mol Cell Endocrinol 2013;365:174-86

29. Eaton SL, Roche SL, Llavero Hurtado M, et al. Total protein analysis as a reliable loading control for quantitative fluorescent Western blotting. PLoS One 2013;8:1-9

30. Li R, Shen Y. An old method facing a new challenge: re-visiting housekeeping proteins as internal reference control for neuroscience research. Life Sci 2013;92:747-51

31. Aldridge GM, Podrebarac DM, Greenough WT, et al. The use of total protein stains as loading controls: an alternative to high-abundance single-protein controls in semi-quantitative immunoblotting. J Neurosci Methods 2008;172:250-4

32. Mukhopadhyay R, Kumar S, Hoh JH. Molecular mechanisms for organizing the neuronal cytoskeleton. Bioessays 2004;26:1017-25

33. Yuan A, Rao MV, Veeranna, et al. Neurofilaments at a glance. J Cell Sci 2012;125:3257-63

34. Ouda L, Druga R, Syka J. Distribution of SMI-32-immunoreactive neurons in the central auditory system of the rat. Brain Struct Funct 2012;217:19-36

35. Triolo D, Dina G, Taveggia C, et al. Vimentin regulates peripheral nerve myelination. Development 2012;139:1359-67

36. Jouhilahti EM, Peltonen S, Peltonen J. Class III beta-tubulin is a component of the mitotic spindle in multiple cell types. J Histochem Cytochem 2008;56:1113-9

37. Hammond JW, Cai D, Verhey KJ. Tubulin modifications and their cellular functions. Curr Opin Cell Biol 2008;20:71-6

38. Black MM, Baas PW, Humphries S. Dynamics of alpha-tubulin deacetylation in intact neurons. J Neurosci 1989;9:358-68

39. Lee G, Rook SL. Expression of tau protein in non-neuronal cells: microtubule binding and stabilization. J Cell Sci 1992;102 (Pt 2):227-37

40. Johnson GV, Stoothoff WH. Tau phosphorylation in neuronal cell function and dysfunction. J Cell Sci 2004;117:5721-9

41. Avila J. Tau phosphorylation and aggregation in Alzheimer's disease pathology. FEBS Lett 2006;580:2922-7

42. Corfas G, Velardez MO, Ko CP, et al. Mechanisms and roles of axon-Schwann cell interactions. J Neurosci 2004;24:9250-60

43. Auld DS, Robitaille R. Perisynaptic Schwann cells at the neuromuscular junction: nerve- and activity-dependent contributions to synaptic efficacy, plasticity, and reinnervation. Neuroscientist 2003;9:144-57

44. Salzer JL. Axonal regulation of Schwann cell ensheathment and myelination. J Peripher Nerv Syst 2012;17 Suppl 3:14-9

45. Misgeld T, Burgess RW, Lewis RM, et al. Roles of neurotransmitter in synapse formation: development of neuromuscular junctions lacking choline acetyltransferase. Neuron 2002;36:635-48

46. Hanada K, Kishimoto S, Bellier JP, et al. Peripheral choline acetyltransferase in rat skin demonstrated by immunohistochemistry. Cell Tissue Res 2013;351:497-510

47. Govindasamy L, Pedersen B, Lian W, et al. Structural insights and functional implications of choline acetyltransferase. J Struct Biol 2004;148:226-35

48. Schliebs R, Arendt T. The cholinergic system in aging and neuronal degeneration. Behav Brain Res 2011;221:555-63

49. Ryter SW, Mizumura K, Choi AM. The Impact of Autophagy on Cell Death Modalities. Int J Cell Biol 2014;2014:1-12

50. Mizumura K, Choi AM, Ryter SW. Emerging role of selective autophagy in human diseases. Front Pharmacol 2014;5:1-8

51. Myeku N, Figueiredo-Pereira ME. Dynamics of the degradation of ubiquitinated proteins by proteasomes and autophagy: association with sequestosome 1/p62. J Biol Chem 2011;286:22426-40

52. Barth S, Glick D, Macleod KF. Autophagy: assays and artifacts. J Pathol 2010;221:117-24

53. Castillo K, Valenzuela V, Matus S, et al. Measurement of autophagy flux in the nervous system in vivo. Cell Death Dis 2013;4:1-11

54. Mizushima N, Yoshimori T. How to interpret LC3 immunoblotting. Autophagy 2007;3:542-5

55. Eskelinen EL. Roles of LAMP-1 and LAMP-2 in lysosome biogenesis and autophagy. Mol Aspects Med 2006;27:495-502

56. Eskelinen EL, Tanaka Y, Saftig P. At the acidic edge: emerging functions for lysosomal membrane proteins. Trends Cell Biol 2003;13:137-45

57. Huynh KK, Eskelinen EL, Scott CC, et al. LAMP proteins are required for fusion of lysosomes with phagosomes. EMBO J 2007;26:313-24

58. Eskelinen EL, Reggiori F, Baba M, et al. Seeing is believing: the impact of electron microscopy on autophagy research. Autophagy 2011;7:935-56

59. Eskelinen EL. To be or not to be? Examples of incorrect identification of autophagic compartments in conventional transmission electron microscopy of mammalian cells. Autophagy 2008;4:257-60

60. Vital A, Meissner WG, Canron MH, et al. Intra-axonal protein aggregation in the peripheral nervous system. J Peripher Nerv Syst 2014;19:44-9

61. Ceballos D, Cuadras J, Verdu E, et al. Morphometric and ultrastructural changes with ageing in mouse peripheral nerve. J Anat 1999;195 (Pt 4):563-76

62. Verdu E, Ceballos D, Vilches JJ, et al. Influence of aging on peripheral nerve function and regeneration. J Peripher Nerv Syst 2000;5:191-208

63. Lee S, Notterpek L. Dietary restriction supports peripheral nerve health by enhancing endogenous protein quality control mechanisms. Exp Gerontol 2013;48:1085-90

64. Chittoor VG, Sooyeon L, Rangaraju S, et al. Biochemical characterization of protein quality control mechanisms during disease progression in the C22 mouse model of CMT1A. ASN Neuro 2013;5:333-46

65. Lee SM, Chin LS, Li L. Protein misfolding and clearance in demyelinating peripheral neuropathies: Therapeutic implications. Commun Integr Biol 2012;5:107-10

66. Yuan A, Sasaki T, Kumar A, et al. Peripherin is a subunit of peripheral nerve neurofilaments: implications for differential vulnerability of CNS and peripheral nervous system axons. J Neurosci 2012;32:8501-8

67. Holzbaur EL, Scherer SS. Microtubules, axonal transport, and neuropathy. N Engl J Med 2011;365:2330-2

68. Chevalier-Larsen E, Holzbaur EL. Axonal transport and neurodegenerative disease. Biochim Biophys Acta 2006;1762:1094-108

69. Cifuentes-Diaz C, Nicole S, Velasco ME, et al. Neurofilament accumulation at the motor endplate and lack of axonal sprouting in a spinal muscular atrophy mouse model. Hum Mol Genet 2002;11:1439-47

70. Mendonca DM, Chimelli L, Martinez AM. Quantitative evidence for neurofilament heavy subunit aggregation in motor neurons of spinal cords of patients with amyotrophic lateral sclerosis. Braz J Med Biol Res 2005;38:925-33

71. Dale JM, Garcia ML. Neurofilament Phosphorylation during Development and Disease: Which Came First, the Phosphorylation or the Accumulation? J Amino Acids 2012;2012:382107

72. Zhang Y, Tian Q, Zhang Q, et al. Hyperphosphorylation of microtubule-associated tau protein plays dual role in neurodegeneration and neuroprotection. Pathophysiology 2009;16:311-6

73. Holzer M, Holzapfel HP, Krohn K, et al. Alterations in content and phosphorylation state of cytoskeletal proteins in the sciatic nerve during ageing and in Alzheimer's disease. J Neural Transm 1999;106:743-55

74. Takahashi S, Saito T, Hisanaga S, et al. Tau phosphorylation by cyclin-dependent kinase 5/p39 during brain development reduces its affinity for microtubules. J Biol Chem 2003;278:10506-15

75. Crespo-Biel N, Theunis C, Van Leuven F. Protein tau: prime cause of synaptic and neuronal degeneration in Alzheimer's disease. Int J Alzheimers Dis 2012;2012:1-13

76. Martin L, Latypova X, Terro F. Post-translational modifications of tau protein: implications for Alzheimer's disease. Neurochem Int 2011;58:458-71

77. Tai HC, Serrano-Pozo A, Hashimoto T, et al. The synaptic accumulation of hyperphosphorylated tau oligomers in Alzheimer disease is associated with dysfunction of the ubiquitin-proteasome system. Am J Pathol 2012;181:1426-35

78. Babu JR, Geetha T, Wooten MW. Sequestosome 1/p62 shuttles polyubiquitinated tau for proteasomal degradation. J Neurochem 2005;94:192-203

79. Paine MG, Babu JR, Seibenhener ML, et al. Evidence for p62 aggregate formation: role in cell survival. FEBS Lett 2005;579:5029-34

80. Kuusisto E, Salminen A, Alafuzoff I. Early accumulation of p62 in neurofibrillary tangles in Alzheimer's disease: possible role in tangle formation. Neuropathol Appl Neurobiol 2002;28:228-37

81. Bilsland LG, Sahai E, Kelly G, et al. Deficits in axonal transport precede ALS symptoms in vivo. Proc Natl Acad Sci U S A 2010;107:20523-8

82. Kasa P, Mann SP, Karcsu S, et al. Transport of choline acetyltransferase and acetylcholinesterase in the rat sciatic nerve: a biochemical and electron histochemical study. J Neurochem 1973;21:431-6

83. Saunders NR, Dziegielewska K, Haggendal CJ, et al. Slow accumulation of choline acetyltransferase in crushed sciatic nerves of the rat. J Neurobiol 1973;4:95-103

84. Haggendal CJ, Saunders NR, Dahlstrom AB. Rapid accumulation of acetylcholine in nerve above a crush. J Pharm Pharmacol 1971;23:552-5

85. Smith DO. Acetylcholine synthesis and release in the extensor digitorum longus muscle of mature and aged rats. J Neurochem 1990;54:1433-9

86. Tucek S. Choline acetyltransferase activity in skeletal muscles after denervation. Exp Neurol 1973;40:23-35

87. Verdier V, Csardi G, de Preux-Charles AS, et al. Aging of myelinating glial cells predominantly affects lipid metabolism and immune response pathways. Glia 2012;60:751-60

88. Amer MG, Mazen NF, Mohamed NM. Role of calorie restriction in alleviation of age-related morphological and biochemical changes in sciatic nerve. Tissue Cell 2014;46:497-504

89. Donato R, Cannon BR, Sorci G, et al. Functions of S100 proteins. Curr Mol Med 2013;13:24-57

90. Chang IA, Oh MJ, Kim MH, et al. Vimentin phosphorylation by Cdc2 in Schwann cell controls axon growth via beta1-integrin activation. FASEB J 2012;26:2401-13

91. Jacobs JM, Love S. Qualitative and quantitative morphology of human sural nerve at different ages. Brain 1985;108 (Pt 4):897-924

92. Tai HC, Schuman EM. Ubiquitin, the proteasome and protein degradation in neuronal function and dysfunction. Nat Rev Neurosci 2008;9:826-38

93. Yi JJ, Ehlers MD. Ubiquitin and protein turnover in synapse function. Neuron 2005;47:629-32

94. Ehlers MD. Activity level controls postsynaptic composition and signaling via the ubiquitin-proteasome system. Nat Neurosci 2003;6:231-42

95. Riley BE, Kaiser SE, Shaler TA, et al. Ubiquitin accumulation in autophagy-deficient mice is dependent on the Nrf2-mediated stress response pathway: a potential role for protein aggregation in autophagic substrate selection. J Cell Biol 2010;191:537-52

96. Mizushima N, Levine B. Autophagy in mammalian development and differentiation. Nat Cell Biol 2010;12:823-30

97. Mizushima N. Autophagy. FEBS Lett 2010;584:1279

98. Hegde AN. The ubiquitin-proteasome pathway and synaptic plasticity. Learn Mem 2010;17:314-27

99. Metcalf DJ, Garcia-Arencibia M, Hochfeld WE, et al. Autophagy and misfolded proteins in neurodegeneration. Exp Neurol 2012;238:22-8

100. Rubinsztein DC, DiFiglia M, Heintz N, et al. Autophagy and its possible roles in nervous system diseases, damage and repair. Autophagy 2005;1:11-22

101. Wong E, Cuervo AM. Autophagy gone awry in neurodegenerative diseases. Nat Neurosci 2010;13:805-11

102. Wong E, Cuervo AM. Integration of clearance mechanisms: the proteasome and autophagy. Cold Spring Harb Perspect Biol 2010;2:1-20

103. Lamark T, Kirkin V, Dikic I, et al. NBR1 and p62 as cargo receptors for selective autophagy of ubiquitinated targets. Cell Cycle 2009;8:1986-90

104. Lamark T, Johansen T. Autophagy: links with the proteasome. Curr Opin Cell Biol 2010;22:192-8

105. Komatsu M, Ichimura Y. Physiological significance of selective degradation of p62 by autophagy. FEBS Lett 2010;584:1374-8

106. Bitto A, Lerner CA, Nacarelli T, et al. P62/SQSTM1 at the interface of aging, autophagy, and disease. Age (Dordr) 2014;36:1123-37

107. Bjorkoy G, Lamark T, Brech A, et al. p62/SQSTM1 forms protein aggregates degraded by autophagy and has a protective effect on huntingtin-induced cell death. J Cell Biol 2005;171:603-14

108. Fetalvero KM, Yu Y, Goetschkes M, et al. Defective autophagy and mTORC1 signaling in myotubularin null mice. Mol Cell Biol 2013;33:98-110

109. McMahon CD, Chai R, Radley-Crabb HG, et al. Lifelong exercise and locally produced insulin-like growth factor-1 (IGF-1) have a modest influence on reducing age-related muscle wasting in mice. Scand J Med Sci Sports 2014;24:423-35

110. Soffe Z, Radley-Crabb HG, McMahon C, et al. Effects of loaded voluntary wheel exercise on performance and muscle hypertrophy in young and old male C57Bl/6J mice. Scand J Med Sci Sports 2015:1-17

111. Manini TM, Hong SL, Clark BC. Aging and muscle: a neuron's perspective. Curr Opin Clin Nutr Metab Care 2013;16:21-6

112. Sakellariou GK, Davis CS, Shi Y, et al. Neuron-specific expression of CuZnSOD prevents the loss of muscle mass and function that occurs in homozygous CuZnSOD-knockout mice. FASEB J 2014;28:1666-81

113. Sataranatarajan K, Qaisar R, Davis C, et al. Neuron specific reduction in CuZnSOD is not sufficient to initiate a full sarcopenia phenotype. Redox Biol 2015;5:140-8

Tables

Table 1**:** Primary antibodies used in this study (IB= immunoblot, IF= immunofluorescence)

Host	Antigen	Source and product number	Dilution	
			IB	IF
Mouse	SMI-32	Covance; SMI-32R, USA	1:1000	1:1000
Rabbit	β-3 Tubulin	Covance; PRB-435P, USA	1:5000	1:5000
Goat	Cholineacetyltransferase	Chemicon; AB144P, USA	1:1000	1:1000
Griffonia Simplicifolia	Isolectin B4-FITC	Vector laboratories; FL-1201, USA		1:100
Mouse	Vimentin	Boehringer; 1112457, Germany	1:1000	
Mouse	Tau-5	Biosource International; AHB0042, USA	1:500	1:500
Mouse	S100(βsubunit)	Sigma Aldrich; S-2532, Australia	1:1000	
Rabbit	SQSTM1/p62	Cell Signalling; 5114, USA	1:1000	
Rabbit	SQSTM1/p62	Cell Signalling; 7695, USA		1:400
Rabbit	LC3B	Cell Signalling; 2775, USA	1:1000	
Rabbit	LAMP-1	Cell Signalling; 3243, USA	1:1000	

Table 2: Secondary antibodies for immunoflourescence

Secondary Antibody	Source and product number	Dilution
Anti-Goat Alexa Fluor 488	Life Technologies; A-11055, Australia	1:1000
Anti Mouse-FITC	MP Biochemicals ; 55521, USA	1:100
Anti -rabbit -Cy3	Jackson ImmunoResearch Labs ; 111-166-006, USA	1:400

Table 3: HRP conjugated secondary antibodies for immunoblotting

Secondary Antibody	Source and product number	Dilution
Anti-Goat F(ab)2 Fragment Specific	Pierce; 31403, USA	1:10000
Anti Mouse IgG (H+L)	Pierce; 31430, USA	1:10000
Anti –Rabbit IgG (H+L)	Pierce; 31460, USA	1:10000

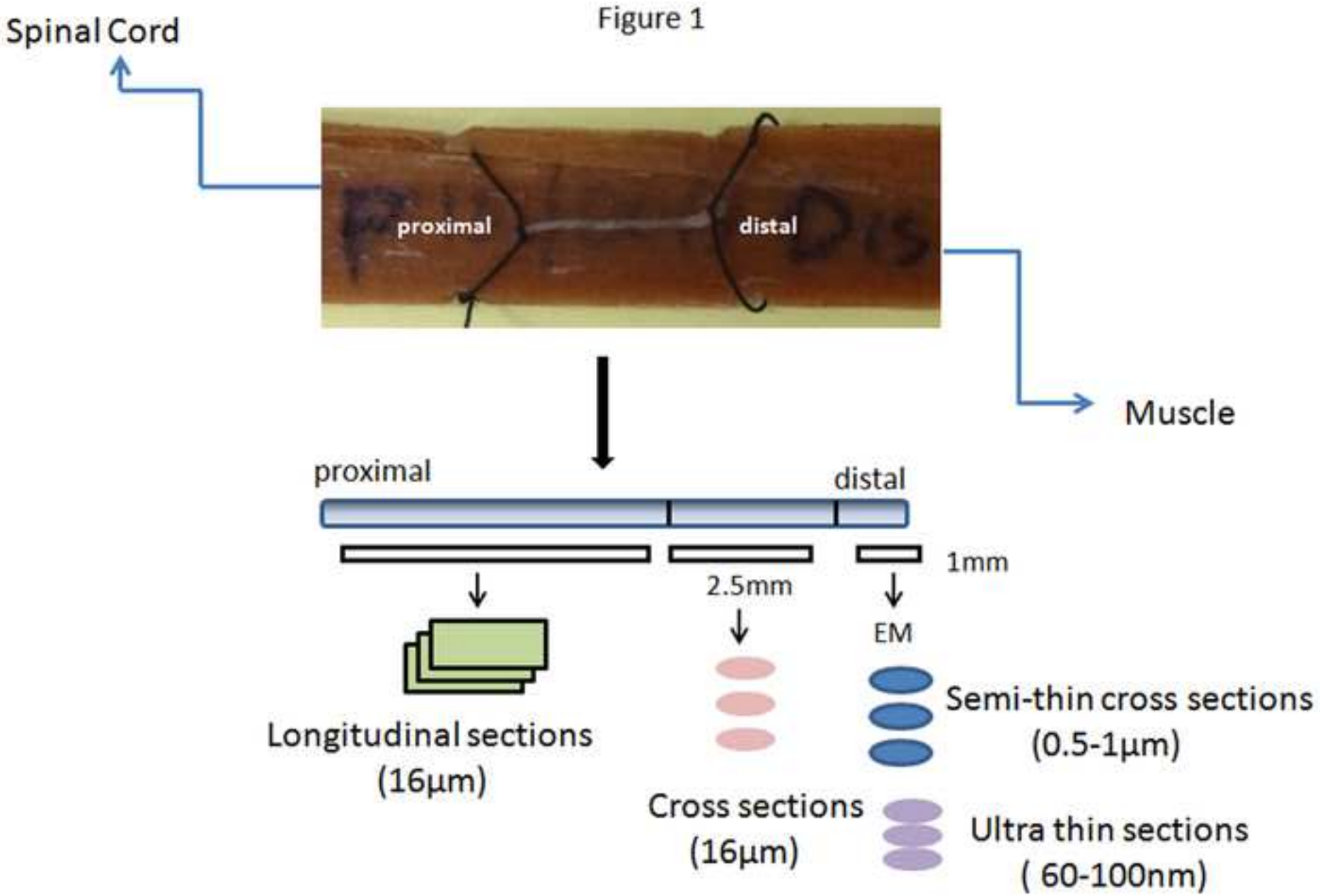

Figure 2

Click here to download Figure Figure 2.tif

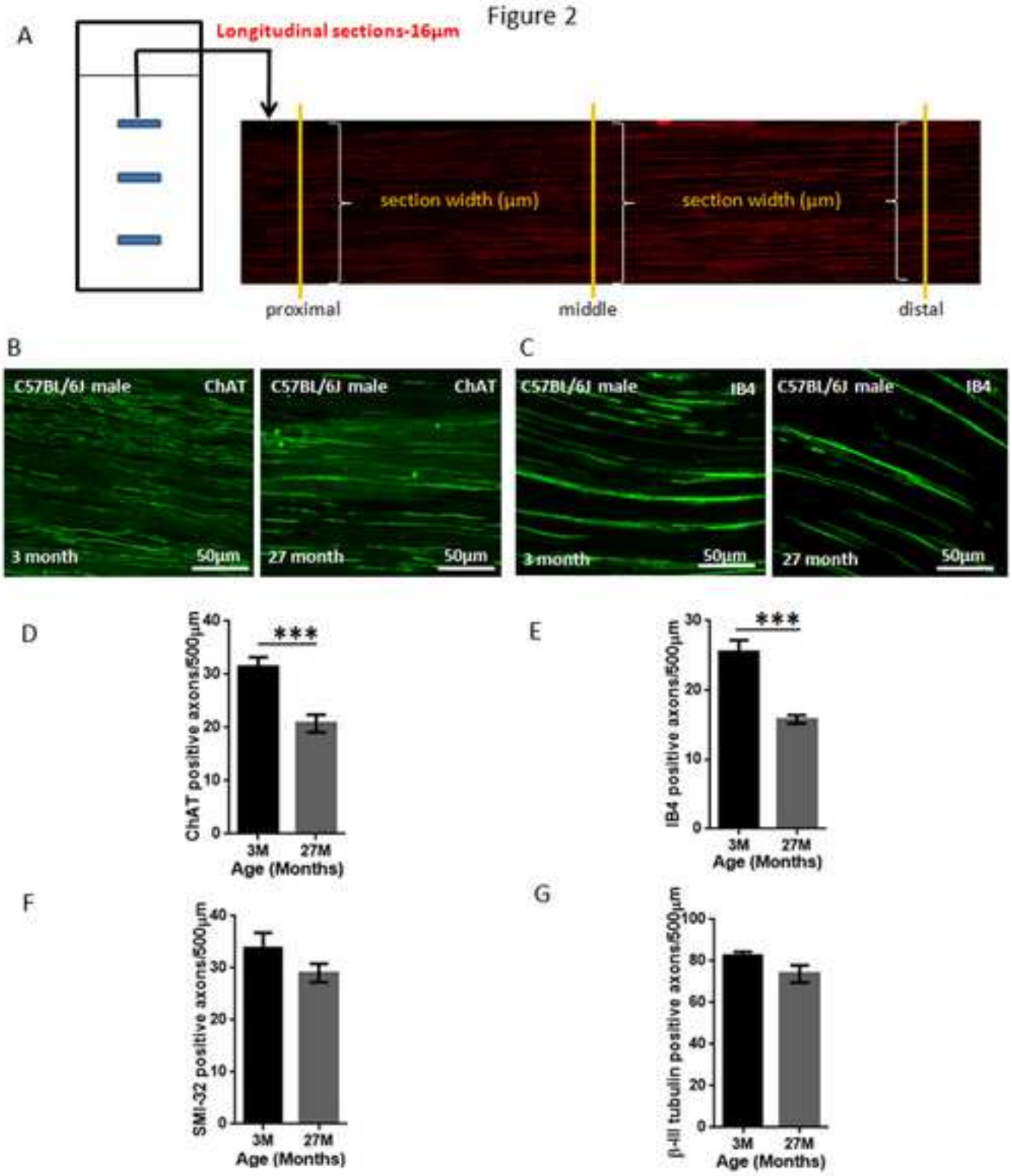

Figure 3

Click here to download Figure Figure 3.tif

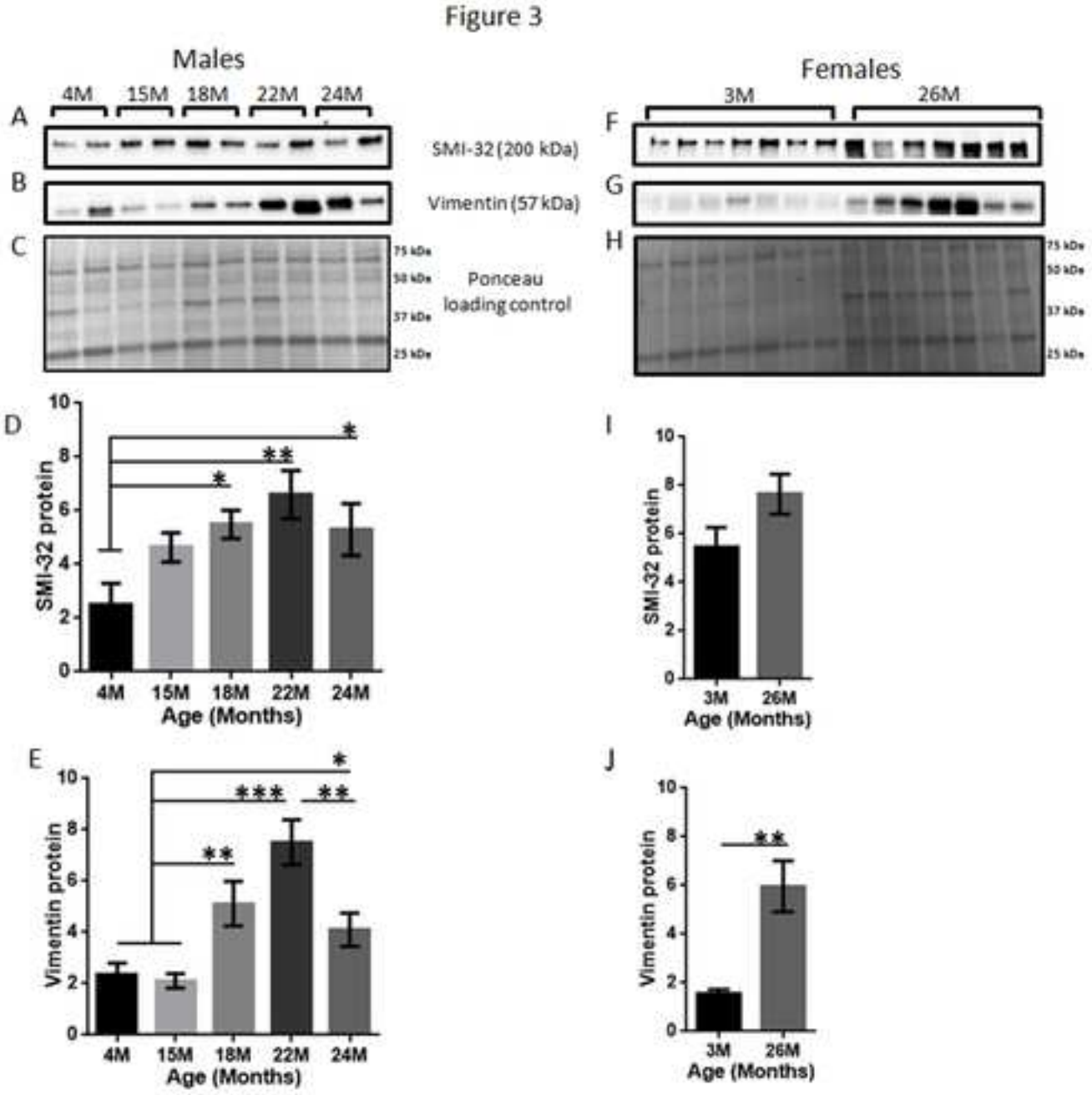

Figure 4

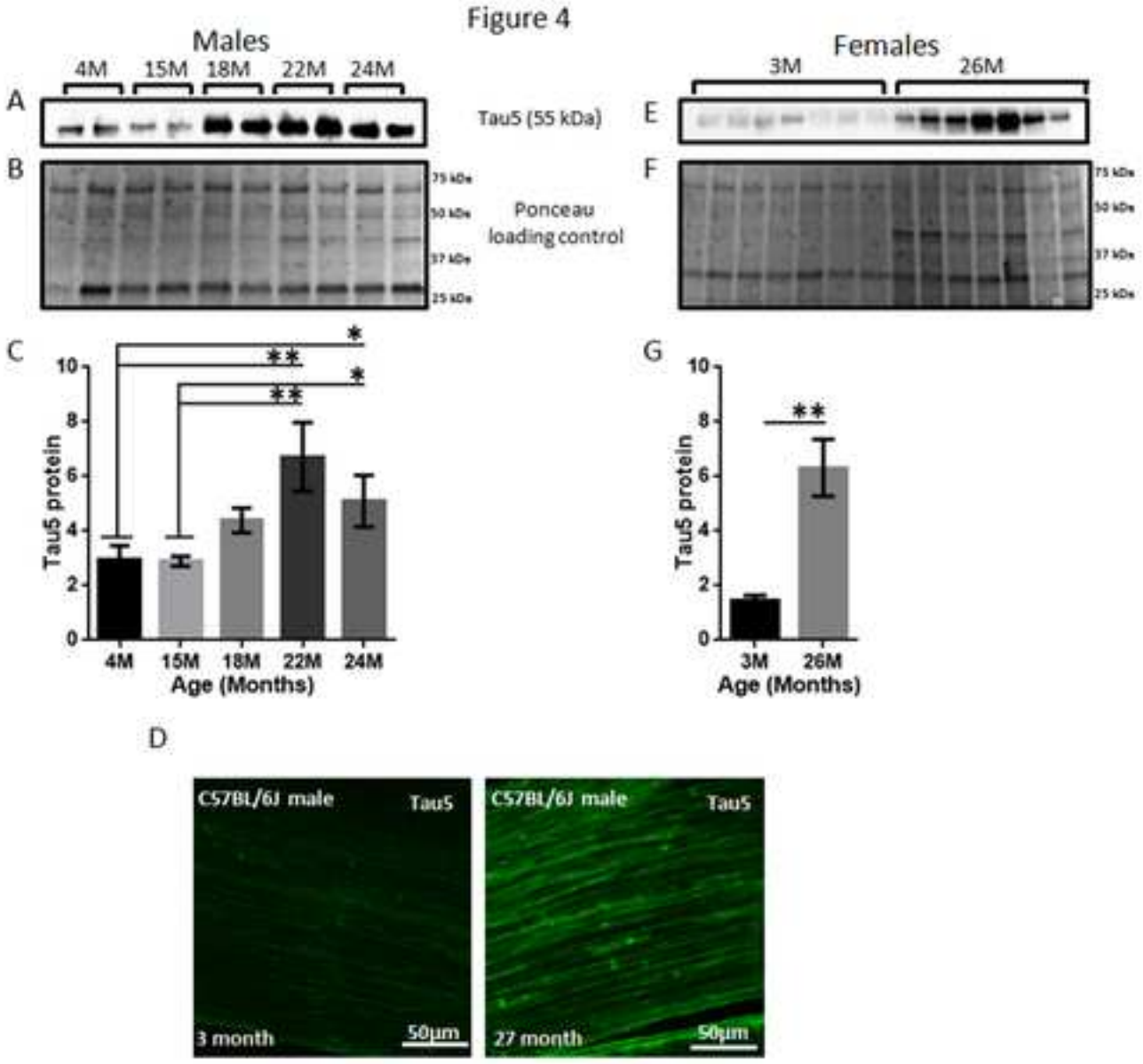

Figure 5

Click here to download Figure Figure 5.tif

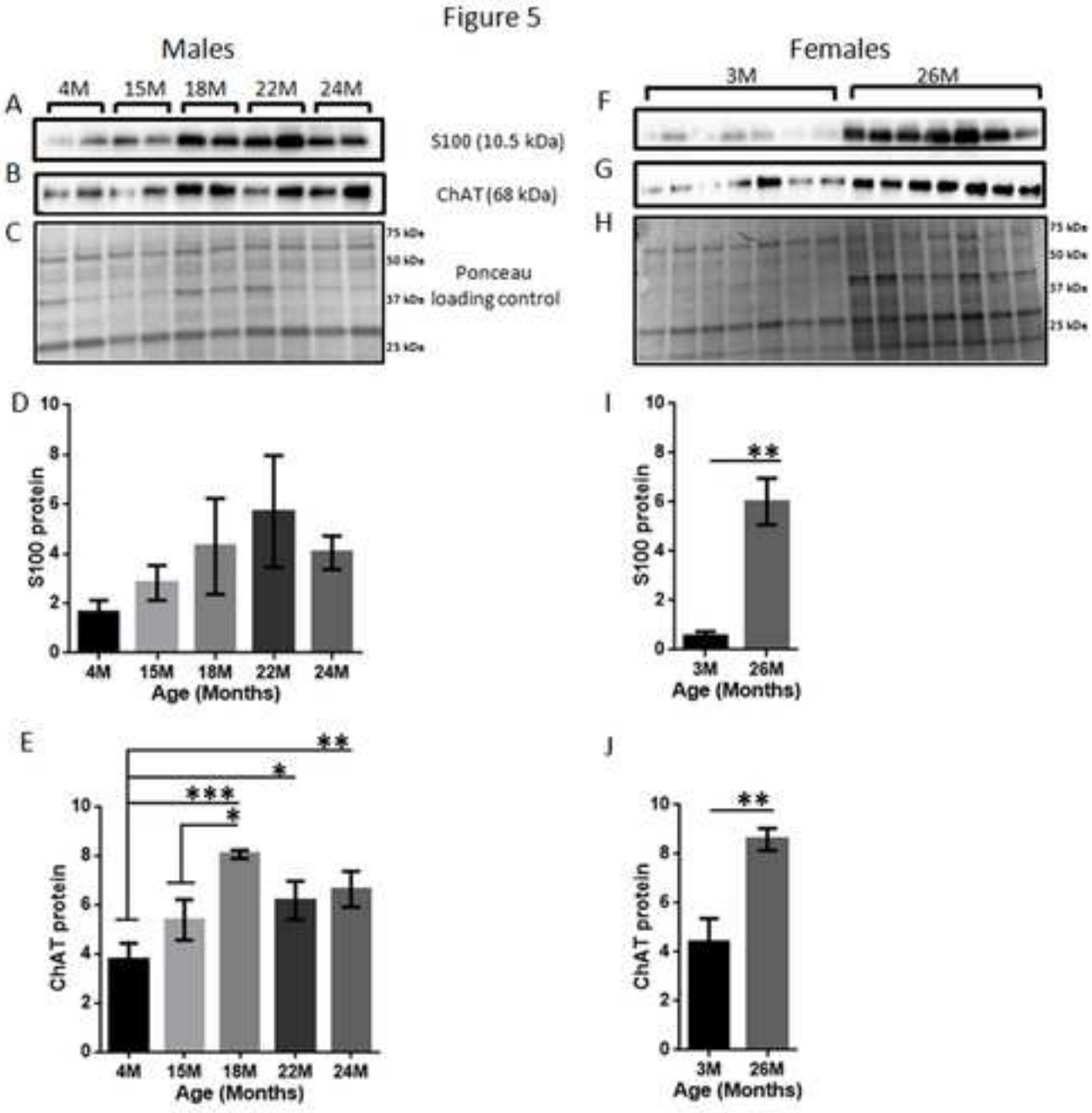

Figure 6

Click here to download Figure Figure 6.tif

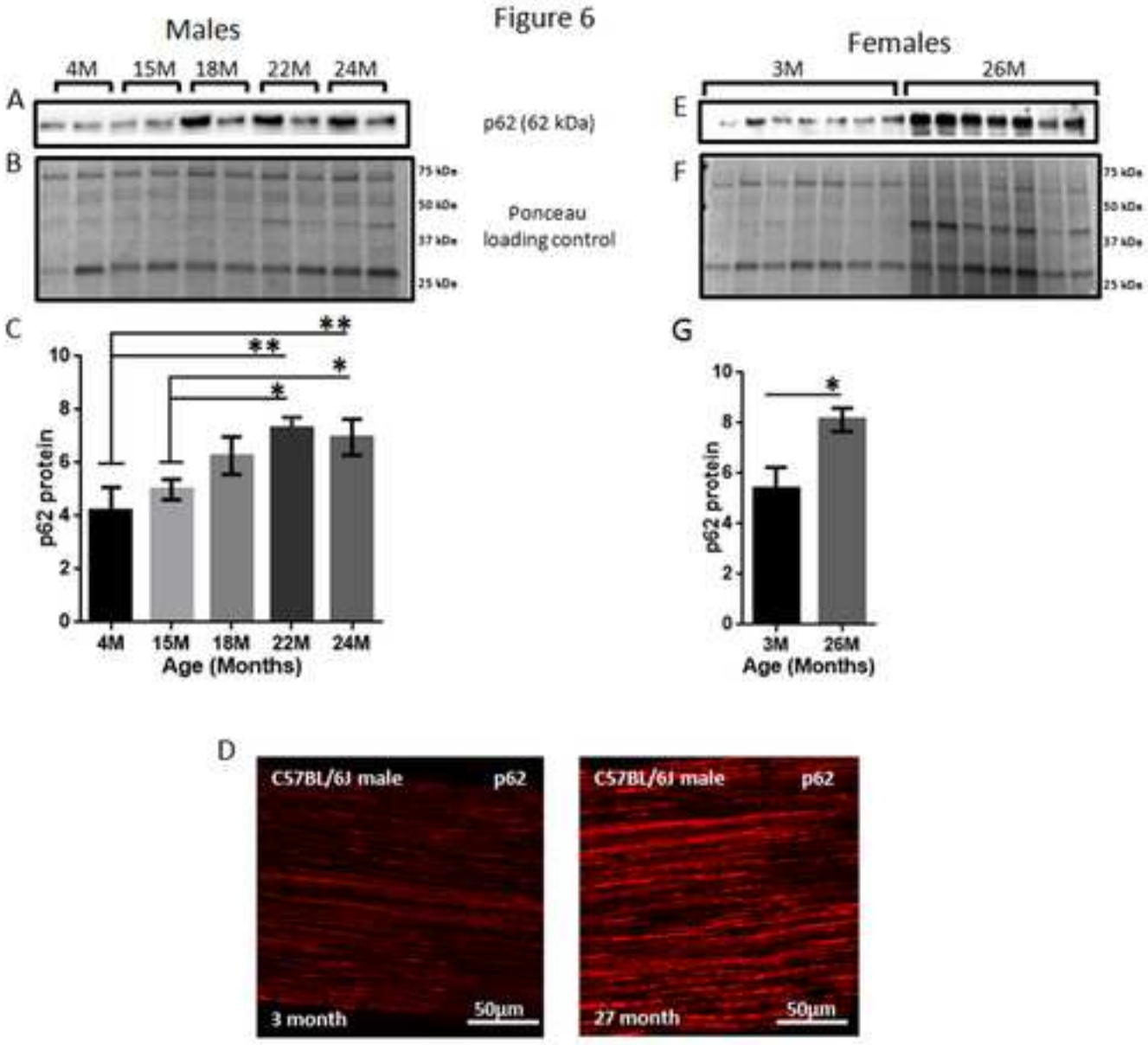

Figure 7

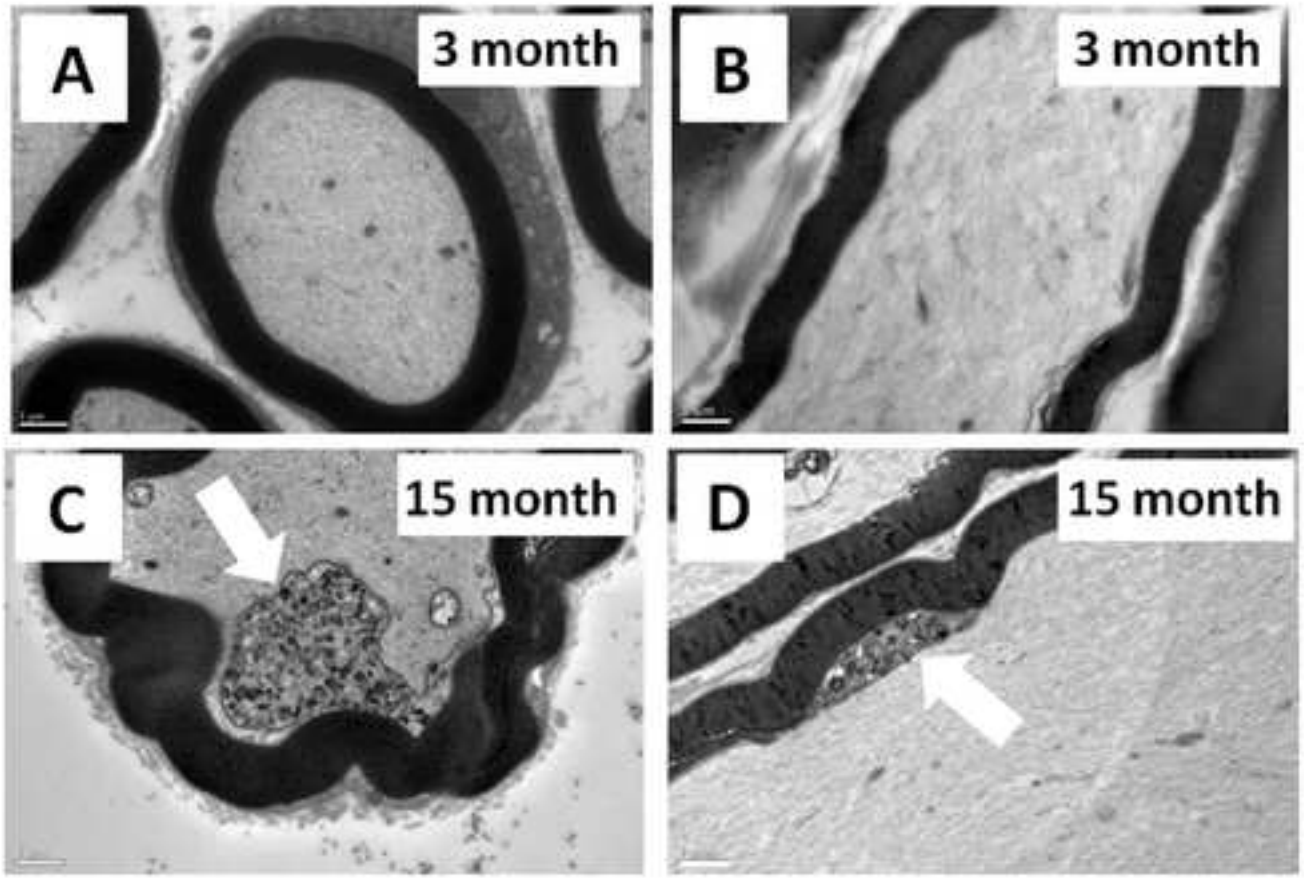

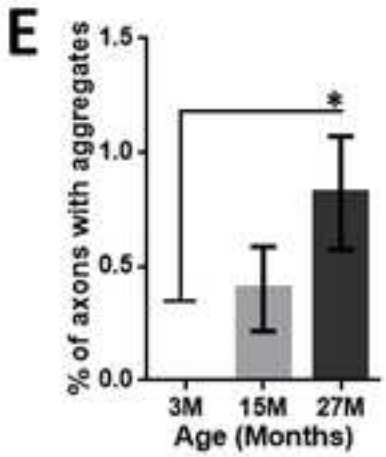

Supplementary Figure 1

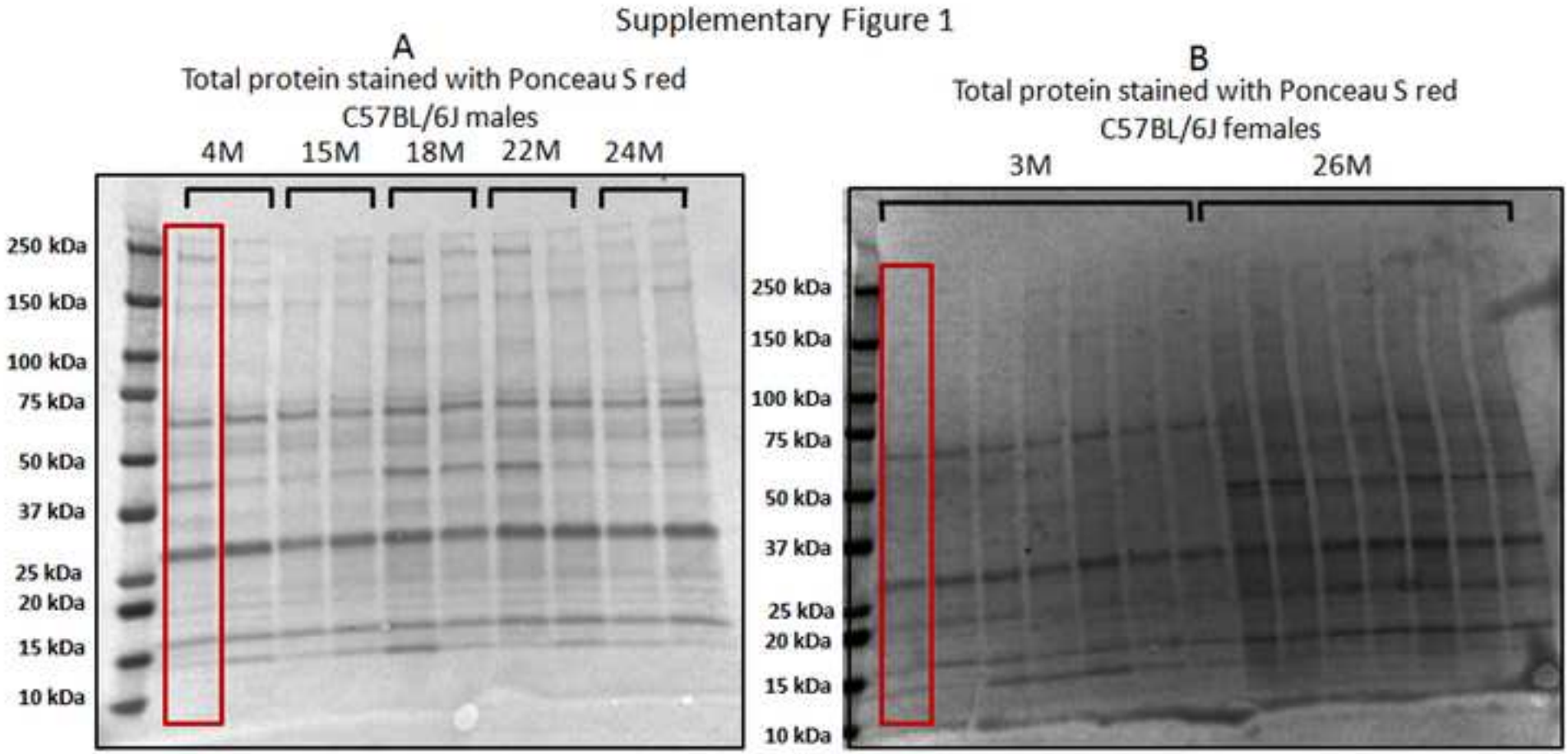

Supplementary Figure 2

Click here to download Figure Supplementary Figure 2.tif

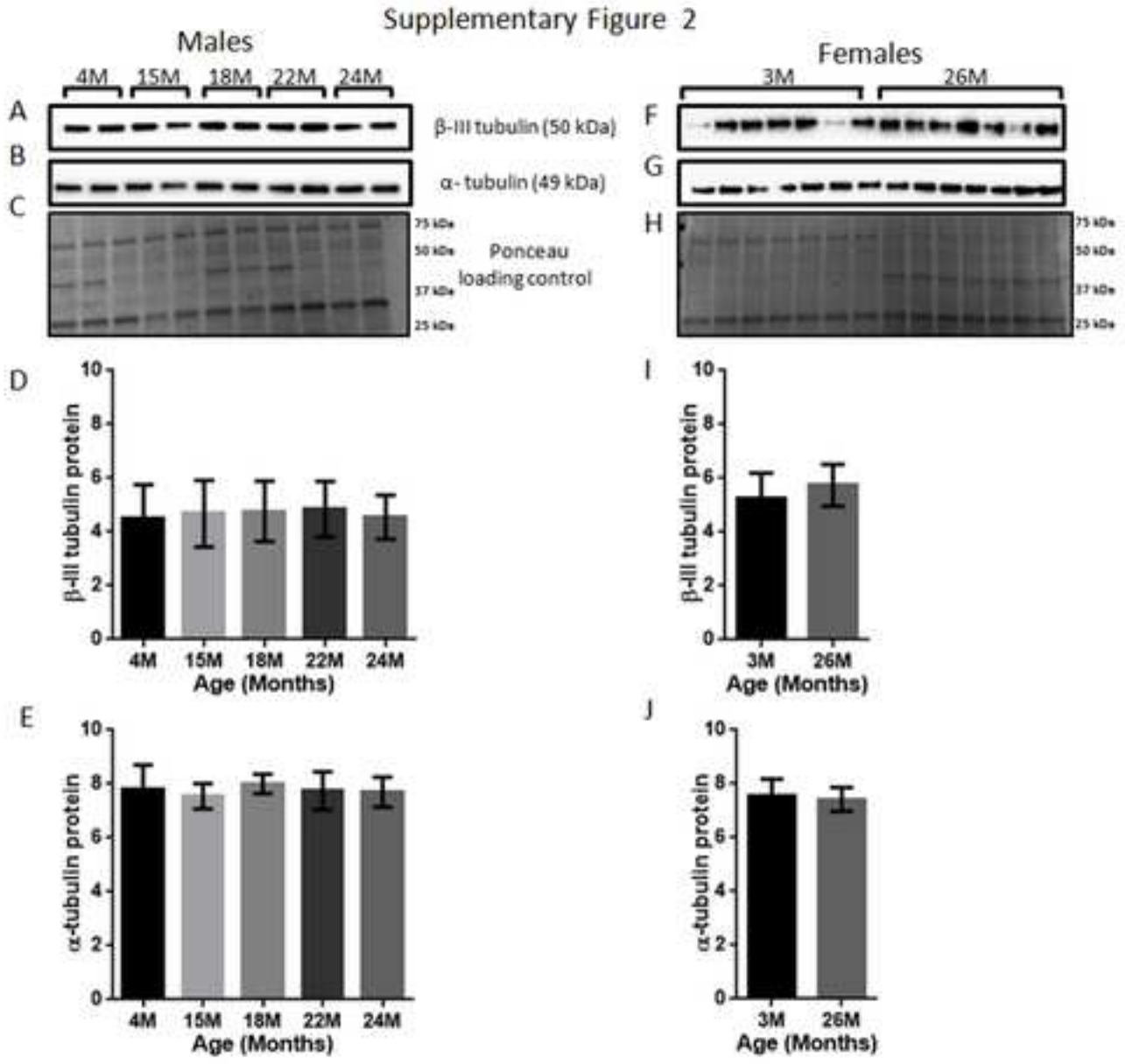

Supplementary Figure 3

Click here to download Figure Supplementary Figure 3.tif

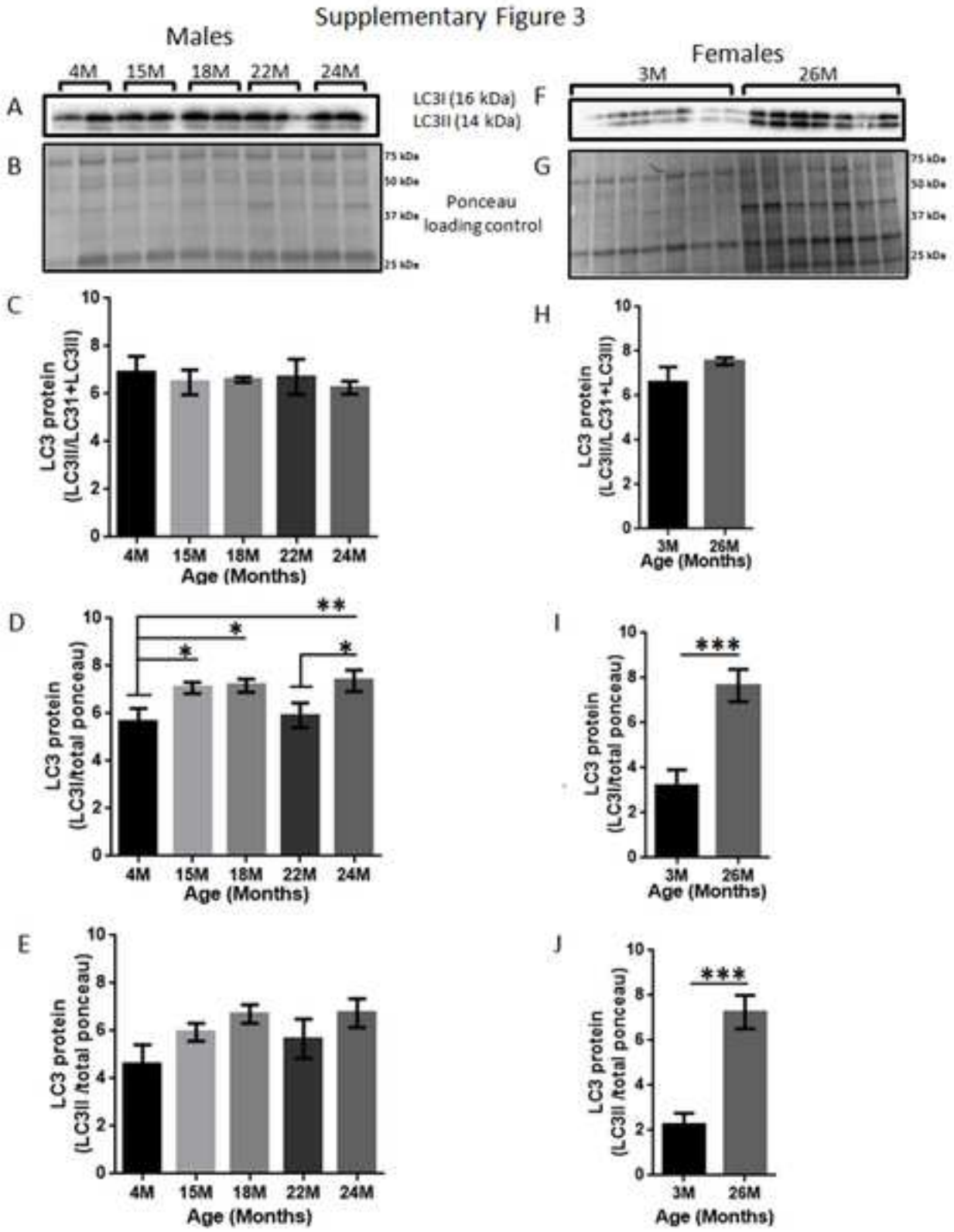

Supplementary Figure 4 Click here to download Figure Supplementary Figure 4.tif